

Review

# Synthesis Methods and Favorable Conditions for Spherical Vaterite Precipitation: A Review

Donata Konopacka-Lyskawa 

Department of Process Engineering and Chemical Technology, Faculty of Chemistry,  
Gdańsk University of Technology, Narutowicza 11/12, 80-233 Gdańsk, Poland;  
donata.konopacka-lyska@pg.edu.pl; Tel.: +48-58-347-2910

Received: 15 March 2019; Accepted: 18 April 2019; Published: 25 April 2019



**Abstract:** Vaterite is the least thermodynamically stable anhydrous calcium carbonate polymorph. Its existence is very rare in nature, e.g., in some rock formations or as a component of biominerals produced by some fishes, crustaceans, or birds. Synthetic vaterite particles are proposed as carriers of active substances in medicines, additives in cosmetic preparations as well as adsorbents. Also, their utilization as a pump for microfluidic flow is also tested. In particular, vaterite particles produced as polycrystalline spheres have large potential for application. Various methods are proposed to precipitate vaterite particles, including the conventional solution-solution synthesis, gas-liquid method as well as special routes. Precipitation conditions should be carefully selected to obtain a high concentration of vaterite in all these methods. In this review, classical and new methods used for vaterite precipitation are presented. Furthermore, the key parameters affecting the formation of spherical vaterite are discussed.

**Keywords:** vaterite; calcium carbonate; polymorph; precipitation; synthesis; carbonation

## 1. Introduction

Vaterite is the least thermodynamically stable anhydrous calcium carbonate polymorph and it easily transforms into more stable calcite or aragonite in the presence of water. This form of calcium carbonate mineral was named to honor the German chemist and mineralogist, Heinrich Vater, in 1903.

Because of its instability, the existence of vaterite is very rare in nature. It has been found in some sediments and rocks [1], e.g., as a major constituent of a carbonated calcium silicate hydrogel complex formed from larnite in Ballycraigy, Ireland [2]. Vaterite can be precipitated in some mineral springs when specific glacial conditions take place [3]. Also, vaterite crystals have been identified in materials produced by living organisms, e.g., otolith organs of fishes [4–6], spicules of the ascidian *Herdmania momus* [6,7], freshwater pearls, crustacean tissues, or bird eggs [6,8] as well as the chalky crust on the surface of leaves of the alpine plant, *Saxifraga scardica* [9].

Synthetic vaterite particles have been used as a carrier of active compounds for medical treatments [10–14]. They have been tested as a template for biodegradable polymer capsules, which can be used for applications in nanomedicine [10,11,15]. Also, vaterite particles are added to personal care products as abrasives, adsorbents, anticaking agents, buffers, or dyes [15]. Due to their unique optical properties, vaterite microspheres have been useful in microrheology and microfluidics [16]. Spherical vaterite particles have been used to generate flow within microfluidic channels that has allowed the creation of an optical driven pump [17]. This polymorphic  $\text{CaCO}_3$  form has been proposed as a coating pigment for ink jet paper [18]. The main advantages of vaterite particles are their easy and low-cost preparation, ability to design particles with defined characteristics, porous structure, mild conditions for decomposition, non-toxicity, and biocompatibility [11,15].

Recently, this unstable mineral was widely investigated to identify the favorable conditions for its production as well as to verify its usefulness for various applications. Therefore, the current opinions on vaterite synthesis as well as a discussion on the variables affecting its formation are overviewed. The issues raised in this review are presented in the diagram in Figure 1.

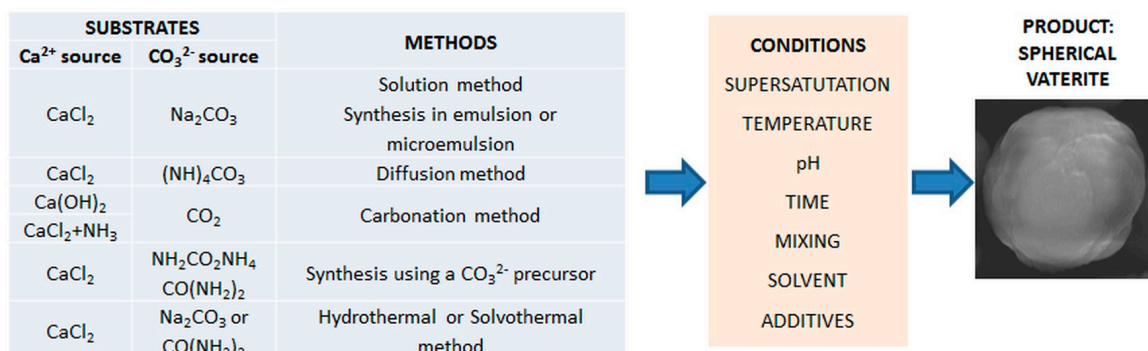


Figure 1. Diagrammatic representation of raised issues.

## 2. Vaterite Properties

Synthetic vaterite particles are usually produced as polycrystalline spheres. The main advantages of such particles' morphology are the porous structure, large surface area, and greater hydrophilicity in comparison to more stable calcite or aragonite [10,19,20]. Other morphological forms of vaterite can be also obtained, i.e., plates [21], hexagonal crystals [22], lenses [23], lamellar aggregates [24], florets, or rosettes [21,25] as well as microtablets [26]. Examples of vaterite particles are shown in Figure 2.

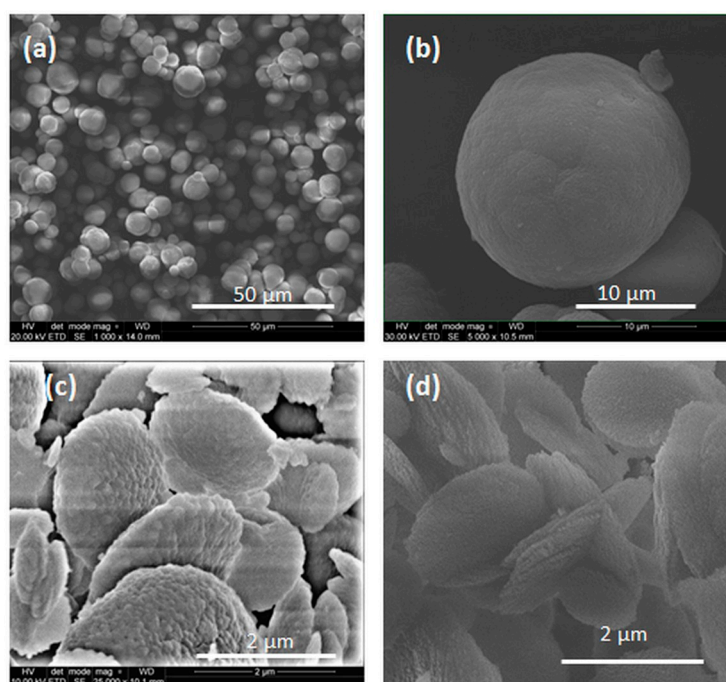


Figure 2. Vaterite particles: (a) and (b) typical spherical particles; (c) spherical and lens-like particles; (d) deformed lens-like and crossed lens-like particles.

Vaterite has a hexagonal crystal system, but the exact crystal structure of vaterite is still under discussion. The analysis of experimental data is consistent in that all vaterite structures belong to the order-disorder (OD) family [27]. It means that the occurrence of multiple polytypes on the micro-to macroscopic scale, as well as considerable stacking disorder, are both to be expected. Recently

Burgess and Bryce [28] used the combined  $^{43}\text{Ca}$  solid-state nuclear magnetic resonance spectroscopic and computational method to indicate two crystal structures, i.e., the hexagonal lattice,  $P3_221$ , and monoclinic lattice,  $C2$ , which have the best agreement between the simulated spectra and diffractograms with the experimental data.

Selected properties of the vaterite are summarized in Table 1.

**Table 1.** Selected properties of vaterite.

| Properties                         | Values  | Ref. |
|------------------------------------|---|------|
| Density                            | 2.54 g/cm <sup>3</sup>  | [2]  |
|                                    | 2.65 g/cm <sup>3</sup>  | [27] |
| $K_{sp}^1$ at 25 °C                | $1.22 \cdot 10^{-8}$  | [29] |
| $K_{sp}$ for $t = 0\text{--}90$ °C | $K_{sp} = -172.1495 - 0.077993T + 3074.688/T + 71.595 \log T$           | [29] |
| Optical properties                 | Semitransparent, colorless  | [17] |
| Effective birefringence            | $\Delta n = 0.06\text{--}0.1$   | [17] |
| Refractive index                   | $n_{\omega} = 1.55, n_{\epsilon} = 1.65$                                | [27] |
| $\alpha_V^2$ at 25 °C              | $35.5 \cdot 10^{-6} \text{ K}^{-1}$                                     | [30] |
| Surface energy                     | Calculated: 90 mJ/m <sup>2</sup> ; experimental 34–73 mJ/m <sup>2</sup> | [31] |

<sup>1</sup> Solubility product; <sup>2</sup> Volumetric thermal expansion coefficient.

The surface of the vaterite particles is usually hydrophilic. The hydrophobic vaterite can be obtained by the adsorption of amphiphilic molecules, e.g., oleic acid, at the interface of the produced vaterite [32]. The charge of vaterite particles depends on the composition of the solution and its pH. The values of the  $\zeta$ -potential were negative when the vaterite particles were dispersed in saturated  $\text{CaCO}_3$  solution at pH 9.0 (−4 mV) and at pH 10.6 (−26 mV) [33]. Another experiment showed that when the solution was composed from 0.01 mol/dm<sup>3</sup>  $\text{CaCl}_2$ , 0.002 mol/dm<sup>3</sup>  $\text{Na}_2\text{CO}_3$ , and 0.5 mol/dm<sup>3</sup>  $\text{NaCl}$ , the charge of the vaterite particles was positive in the range of pH 7.5 to 9.9 [34]. The addition of organic compounds, like polypeptides or fulvic acid, can change the charge of the vaterite particles due to its adsorption at the precipitated crystal interface [33,34].

The mechanical properties of synthetic vaterite particles were determined using nanoindentation analysis [30]. The elastic modulus was found to be in the range of 16 to 61 GPa and the calculated mean value of this parameter was 31 GPa. The determined hardness of vaterite was in the range of 4.2 to 0.3 GPa with a mean value of 0.9 GPa.

During the heating of vaterite particles, thermal transformation and decomposition occurs. The exothermic transformation of vaterite into calcite takes place at temperatures between 395 and 540 °C [6,35,36]. The exact transformation temperature of vaterite into calcite depends on the particle characteristics, the presence of additives, and the heating rate. The shift of the vaterite transformation to a lower temperature may be observed when calcite is present in the sample [35,36] or in the case of the incorporation of organic molecules or foreign ions into the vaterite particles [6,37]. Also, the coexistence of pure vaterite and vaterite in contact with the calcite phase (e.g., vaterite particles covered by a calcite layer) [36] can cause the appearance of a broad range of transformation temperatures.

Recently, a report on the pressure-induced phase transition of vaterite was presented [38]. With increasing pressure, vaterite transformed to high-pressure vaterite forms (vaterite II, vaterite III, and vaterite IV) or partially to calcite. All phase transitions related to vaterite were reversible, except for vaterite II to calcite III.

The presence of vaterite in calcium carbonate samples can be determined using Fourier transformed infrared spectroscopy (FTIR) [39], powder X-ray diffraction (PXRD), Raman spectroscopy [40], or  $^{43}\text{Ca}$  solid state nuclear magnetic resonance ( $^{43}\text{Ca}$  ssNMR) [41]. Characteristic peaks of calcite, aragonite, and vaterite, obtained in spectra or diffractograms that allow these polymorphic forms to be distinguished by FTIR, XRD, Raman spectroscopy, and  $^{43}\text{Ca}$  ssNMR, are listed in Table 2.

**Table 2.** Characteristic peaks of CaCO<sub>3</sub> polymorphs in FTIR, XRD, Raman spectroscopy, and <sup>43</sup>Ca ssNMR analysis.

| Analytical technique  | Vaterite | Aragonite | Calcite | Ref. |
|---|----------|-----------|---------|------|
| FTIR, Wave number, cm <sup>-1</sup>                         | 745      | 710, 713  | 713     | [39] |
| XRD, 2θ°  | 29.5     | 45.9      | 25.0    | [40] |
| Raman, Wave number, cm <sup>-1</sup>                        | 750      | 705       | 711     | [40] |
| <sup>43</sup> Ca ssNMR, δ <sub>iso</sub> <sup>1</sup> , ppm | −3       | −34       | 6       | [41] |

<sup>1</sup> The isotropic chemical shift.

### 3. Mechanisms of Spherical Vaterite Formation

The crystallization of calcium carbonate crystalline polymorphs often occurs via amorphous calcium carbonate (ACC), which is initially formed in the solution [42]. The structure of the ACC precursor consists of a porous calcium-rich nanoscale framework containing water and carbonate ions. ACC is transformed into vaterite due to the rapid dehydration and internal structure reorganization. It is suggested that the possibility of crystallization of the vaterite particles occurs, as the initially generated ACC exhibits proto-vaterite features. [43]. In the final stage, the slow transformation of vaterite into calcite takes place via a dissolution and recrystallization process [42].

There are two main concepts proposed for the explanation of spherical vaterite formation. The first one is based on the aggregation of nanoparticles and the second mechanism is a development of the classical theory of crystal growth [44]. According to the first concept, the production of polycrystalline vaterite particles is a result of the assembly of nano-sized crystals by oriented or not-oriented attachment [44,45]. The aggregation requires the production of many small particles at the beginning of the reaction, which is supported by a high supersaturation. The aggregation mechanisms were applied to interpret both the formation of core-shell microspheres [45] and hollow vaterite particles [46]. It was suggested that the core-shell vaterite structure was a result of a successive aggregation and coverage of formed spheres with hexagonal plates [45] in the presence of poly(styrene sulfonic acid) sodium salt, while the precipitation with the addition of ethylene glycol led to the formation of an initial shell structure from the primary nanoparticles and then hollow vaterite particles [46].

However, the spherulitic growth mechanism is based on the classical theory of crystal growth [44]. Spherulites are produced when a new nucleus arises on the surface of the growing crystal. Based on the experiments, two concepts of spherical growth are proposed: (i) Spherulites arise from a central precursor via multidirectional growth of crystalline fibers, and (ii) spherules grow from a precursor via low angle branching starting on the edges [44,47]. The spherulitic growth mechanism was used to explain the formation of vaterite particles with spherical and dumbbell morphology [47,48].

### 4. Methods of the Synthesis of Vaterite Particles

#### 4.1. Solution Route (L-L)

In this method, a solution containing calcium salt is mixed with a solution of carbonate salt [49]. When calcium chloride and potassium carbonate solutions are used, the reaction is as follows:



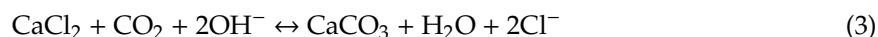
The total volume of the first solution used can be added immediately to the second solution [50,51] or it can be injected to another one with a controlled rate [52]. Different types of stirring are used to produce a homogeneous reaction mixture. Stirrers applied in laboratories are usually mechanical and magnetic, although other types are also proposed, e.g., ultrasound or microwave [13,53]. Recently, a “dropwise precipitation” has been adopted to calcium carbonate precipitation [54]. In this method, a calcium ion solution is added in very small portions to a carbonate solution.

#### 4.2. Carbonation Route (G-L)

Vaterite particles can be synthesized using carbon dioxide as a reagent. The reaction may be carried out using calcium hydroxide or calcium salt as a source of  $\text{Ca}^{2+}$  ions. The reaction of calcium hydroxide and carbon dioxide can be written as:



When gaseous  $\text{CO}_2$  is introduced into the aqueous solution of calcium salt (e.g.,  $\text{CaCl}_2$ ), the overall following reactions can be presented as:



The detailed mechanisms of calcium carbonate precipitation are complex and include the transfer of carbon dioxide from the gas phase into the liquid phase, the formation of a carbonic acid, and its hydrolysis to produce carbonate ions that are the reagent for  $\text{CaCO}_3$  precipitation. The basic pH of the reactive mixture favors both  $\text{CO}_2$  absorption and carbonate ion formation. In case of calcium hydroxide slurry, the initial pH is about 12.4, and therefore the  $\text{CO}_2$  absorption is relatively easy. However, when calcium salts (e.g., calcium chloride,  $\text{CaCl}_2$ , or calcium nitrate,  $\text{Ca(NO}_3)_2$ ) are used, the pH of solution is more acidic and less advantageous to the formation of carbonate ions. Therefore,  $\text{CO}_2$  absorption promoters, like ammonia [19,20,55,56] or amines [56,57], are added to the initial solution. Moreover, carbamate ions that form during carbon dioxide absorption in ammonia and primary or secondary amine aqueous solutions may stabilize the vaterite phase [56,58]. A modification of this approach is the use of extracts obtained by the leaching of calcium to reach minerals or solid waste with ammonium salt solutions [59]. The formed leachates contain calcium ions and ammonia and can be utilized in the carbonation process.

Recently, an interesting synthesis method using solid  $\text{CO}_2$  (dry ice) was proposed [60]. The reaction was carried out at a minimum temperature of  $-50^\circ\text{C}$  in a water-methanol solution containing calcium oxide. The addition of dry ice pellets into a water-methanol solution kept the temperature low and the use of methanol allowed the liquid state of the reaction system to be maintained. Such conditions promoted the  $\text{CO}_2$  solubility and enabled the synthesis of vaterite nanoparticles.

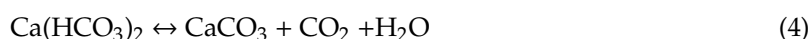
#### 4.3. Diffusion Method

Calcium carbonate in vaterite form can be produced by a diffusion method, in which ammonium carbonate [52] or ammonium bicarbonate [61] is used. These compounds slowly decompose the formed ammonia gas and carbon dioxide. The precipitation is carried out in a closed vessel containing a container with a calcium salt solution and a container with solid carbonates. The formed gases diffuse into the calcium salt solution. After the absorption of ammonia and carbon dioxide, the calcium carbonate is formed in the liquid phase according to the reaction described by Equation (3).

#### 4.4. Synthesis in Emulsions and Microemulsions

The reaction between calcium ions and carbonate ions may take place in the emulsion system. A water-in-oil emulsion containing a single reagent solution as the dispersed phase can be used for the reaction. A second reactant solution is added to the emulsion and precipitation occurs in the dispersed aqueous phase [62]. A stable double water-in-oil-in-water emulsion can be used for vaterite synthesis as well. In this case, calcium ions dissolved in the external phase are extracted into the organic phase containing oil-soluble extractant and stripped into the internal aqueous phase, where the reaction with carbonate ions occurs [63]. Also, the use of microemulsions is proposed for the production of vaterite. For this purpose, two microemulsions containing  $\text{Ca}^{2+}$  and  $\text{CO}_3^{2-}$  ions are prepared. Then, these microemulsions are mixed together to produce calcium carbonate [64].

Another approach to calcium carbonate precipitation in a microemulsion system is the decomposition of calcium bicarbonate:



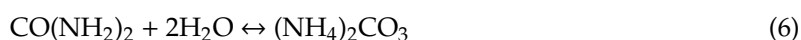
When a saturated solution of calcium bicarbonate is a water phase in a water-in-oil emulsion, vaterite is formed during the slow desorption of carbon dioxide from an aqueous phase. Sponge-like vaterite spheroids were produced using this method [65].

#### 4.5. Synthesis Using a Precursor of Carbonate Ions

The synthesis of calcium carbonate can be carried out using a substance that forms carbonate ions in the reaction environment. Such carbonate ion promoters may be ammonium carbamate [58] or urea [66,67]. Ammonium carbamate hydrolyzes in aqueous solutions to form ammonium carbonate:



Ammonium carbonate is also the product in the reaction of urea with water:



A high concentration of both soluble calcium salts and carbonate ions precursors is necessary to precipitate vaterite polymorph [58,66]. Successful vaterite precipitation has been carried out at temperatures of 15, 25, and 50 °C, when ammonium carbamate has been used [58]. While, the reaction in the solution containing soluble calcium salt and urea required a temperature of 90 °C [66].

#### 4.6. Hydrothermal and Solvothermal Methods

A hydrothermal or solvothermal process is a method used to create ceramic materials at elevated temperatures and pressure. Hydrothermal conditions were applied to precipitate vaterite-reach particles using diethylenetriaminepentaacetic acid as an additive [68]. The first step of this process was  $\text{CaCO}_3$  precipitation using  $\text{CaCl}_2$  and  $\text{Na}_2\text{CO}_3$  solution at a temperature of 120 °C. Then, the hydrothermal process was carried out using the filtrate from the first step as a reactive mixture. The filtrate was placed in an autoclave at temperatures between 130 and 230 °C for 48 hours and the highest concentration of vaterite (90%) was obtained at the highest tested temperature, i.e., 230 °C.

The solvothermal method for vaterite synthesis was proposed by Li et al. [23]. Calcium chloride and urea (a precursor of carbonate ions) were reagents dissolved in ethylene glycol, 1,2-propanediol, or glycerol. Carbonate ions were formed by decomposition of urea in solvothermal conditions at temperatures from 100 to 190 °C for 12 hours. No additives or pH control were needed to precipitate the pure vaterite phase. The pure vaterite particles were produced in ethylene glycol at 100 °C, in 1,2-propanediol at 130 °C, and in glycerol at 150 °C.

### 5. Factors Influencing Vaterite Formation

Calcium carbonate can form several polymorphs, therefore, its crystallization requires careful control of the process parameters to obtain the desired product. Factors affecting the crystallization of the preferred polymorphic form have been grouped by Kitamura in a set of primary and secondary variables [69]. Primary factors include supersaturation, temperature, stirring rate, and seed crystals. However, the solvent composition, additives, and pH are secondary factors. The main investigated factors influencing the precipitation of vaterite are presented below. The effect of solvents and other organic substances is discussed together because organic solvents are treated as additives in many studies on calcium carbonate precipitation.

### 5.1. Supersaturation

Supersaturation is defined as:

$$S = \left( \frac{a_{\text{Ca}^{2+}} a_{\text{CO}_3^{2-}}}{K_{\text{sp}}} \right)^{1/2} \quad (7)$$

where  $a_{\text{Ca}^{2+}}$  and  $a_{\text{CO}_3^{2-}}$  are activities of a calcium and carbonate ions, respectively, and  $K_{\text{sp}}$  is a solubility product. In the liquid-liquid systems, vaterite particles precipitate at room temperature from moderately supersaturated aqueous solutions, i.e., when  $S < 6.5$  [21,33,69,70]. The supersaturation can influence the size of the crystallite forming vaterite particles, and a smaller crystal subunit was observed when supersaturation increased [69,70]. When precipitation is carried out by a carbonation route, the composition of the gas stream can impact on the supersaturation, i.e., an increase in the  $\text{CO}_2$  concentration in the gas phase resulted in the higher supersaturation. The high supersaturation in the buffered pH range (from about 9.5 to 7.7) helps to trap metastable vaterite, preventing its transformation in calcite [19]. Also, more regular spherical particles are produced at higher concentrations of  $\text{CO}_2$  in feed gas mixtures [71].

### 5.2. Temperature

Usually, vaterite particles can be formed in a broad range of temperatures using a solution method of calcium carbonate precipitation [24,42,58,72]. The comparison of vaterite concentrations in calcium carbonate samples precipitated at various conditions is shown in Figure 3. The favored range of temperatures for vaterite precipitation in various experiments is up to 40 °C. This range is also valid when the carbonation route is applied to produce  $\text{CaCO}_3$  in the vaterite form [59,71].

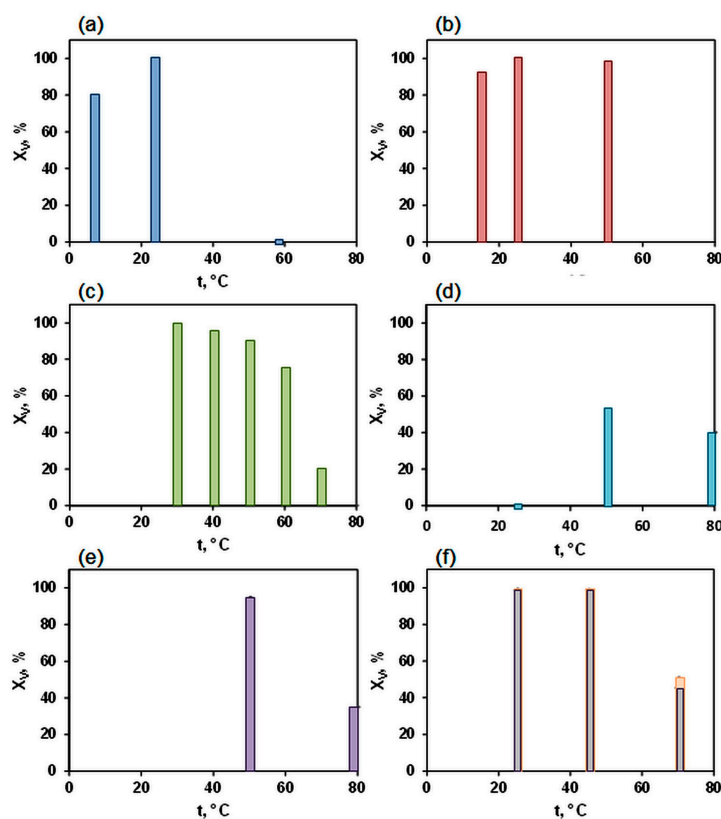


**Figure 3.** Influence of temperature on vaterite concentration in  $\text{CaCO}_3$  samples; (a) L-L,  $S = 6.5$ ,  $\text{pH} = 9$ , based on data from [21]; (b) with carbamate,  $[\text{Ca}^{2+}] = 1.5 \text{ M}$ , based on data from [58]; (c) L-L,  $[\text{Ca}^{2+}] = 0.25 \text{ M}$ , based on data from [24]; (d) L-L,  $[\text{Ca}^{2+}] = 0.015 \text{ M}$  [73]; (e) L-L,  $[\text{Ca}^{2+}] = 0.015 \text{ M}$  with ethylene glycol based on data from [73]; (f) G-L,  $\text{pH} = 9\text{--}10$ ,  $x_{\text{CO}_2} = 1$ ,  $V_G = 50 \text{ dm}^3/\text{h}$  (gray),  $V_G = 100 \text{ dm}^3/\text{h}$  (orange) based on data from [59].

The application of the hydrothermal or solvothermal method allowed the precipitation of vaterite at temperatures above 100 °C [23,68]. Some additives, e.g., ethylene glycol, can promote vaterite formation at temperatures above 40 °C [42]. A higher concentration of vaterite was observed in the CaCO<sub>3</sub> product precipitated in an ethylene glycol-water solution at a temperature of 50 °C compared to the reaction carried out in an aqueous solution (see Figure 3d,e).

### 5.3. pH

The pH value of the reaction mixture is an important parameter during calcium carbonate precipitation. It was reported that vaterite is a dominant polymorph in solutions with an initial basic pH [21,42,74]. However, Han et al. [55] studied a carbonation system with ammonia as an absorption promoter and found that pure vaterite is formed when the pH is 8, but an increase in the pH value of the reactive mixture resulted in a decrease in the vaterite concentration. Almost pure vaterite produced in a gas-liquid system with the addition of ammonia and ammonium chloride was obtained when the pH decreased from 9.7 to 7.7 during the carbonation process [19]. The influence of pH on the vaterite content in selected processes is shown in Figure 4. Vaterite precipitation was promoted in the pH range from 8 to 10 for all compared processes. An extension of this range was possible by conducting precipitation in the presence of ethylene glycol [74] or ionic liquid surfactant [75].

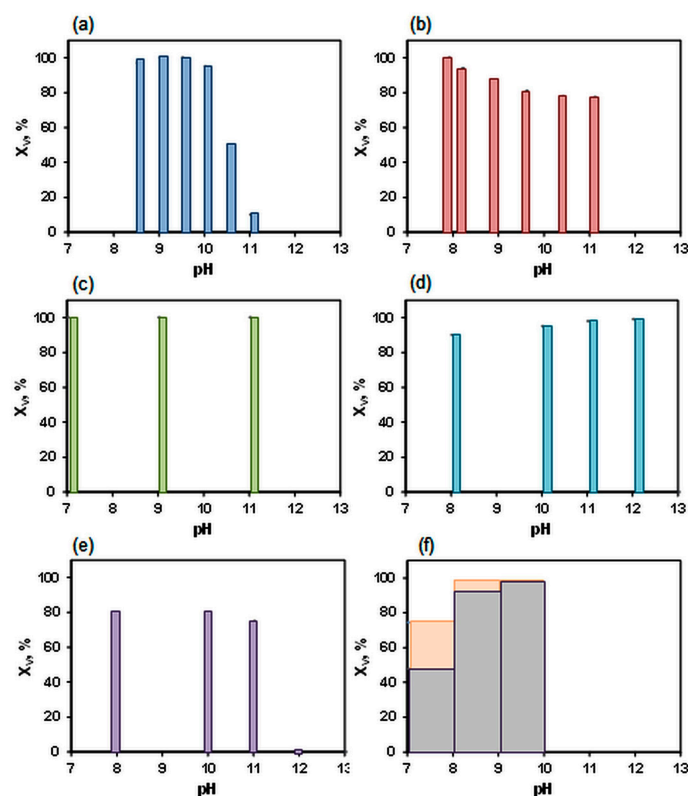


**Figure 4.** Influence of pH on vaterite concentration in CaCO<sub>3</sub> samples; (a) L-L, S = 6.5, t = 24 °C, based on data from [21]; (b) G-L, [Ca<sup>2+</sup>] = 0.1 M, t = 20 °C, V<sub>G</sub> = 18 dm<sup>3</sup>/h, x<sub>CO<sub>2</sub></sub> = 0.33, based on data from [55]; (c) L-L, [Ca<sup>2+</sup>] = 0.5 M, t<sub>a</sub>, with ILS, based on data from [75]; (d) L-L, [Ca<sup>2+</sup>]:[CO<sub>3</sub><sup>2-</sup>] = 1:3, t = 23 °C, with ethylene glycol, based on data from [74]; (e) L-L, [Ca<sup>2+</sup>]:[CO<sub>3</sub><sup>2-</sup>] = 1:1, t = 23 °C, with ethylene glycol, based on data from [74]; (f) G-L, t = 25 °C, x<sub>CO<sub>2</sub></sub> = 1, V<sub>G</sub> = 50 dm<sup>3</sup>/h (gray), V<sub>G</sub> = 100 dm<sup>3</sup>/h (orange), based on data from [59].

### 5.4. Time

Because vaterite is a metastable calcium carbonate polymorph, prolonging the reaction time results in a reduction of the vaterite content when an aqueous solution without the presence of organic



additives is the medium of  $\text{CaCO}_3$  synthesis [13,49]. The remaining precipitated vaterite particles in the aqueous solutions lead its recrystallization to the more stable calcium carbonate polymorph, i.e., aragonite and calcite [58,69]. The time needed for the transformation of vaterite to calcite is usually in the range of a few minutes to several hours [13,58,69,76]. However, a longer time (up to 20 h) of vaterite stability in aqueous solutions was also reported when calcium carbonate was synthesized at a temperature of 7 °C [48]. Slight acceleration of the conversion of vaterite into calcite with an increase of the ionic strength was observed [77]. Some organic compounds used as additives can prevent the transformation of vaterite into calcite (see Section 5.6. Additives).

### 5.5. Mixing

The mixing rate of the reactant solutions is an important factor of the precipitation process [69]. The stirring intensity can affect the activation energy of nucleation of calcite and vaterite in the aqueous system [52]. Local non-homogeneities of the supersaturation can affect the creation of conditions conducive to the formation of one of the polymorphic forms. Homogeneous, high-shear, and constant agitation of reactant solutions enables precipitation of pure vaterite particles [49]. Also, ultrasonic agitation can be used for this purpose [13]. Ultrasounds provide a large amount of energy into the reaction systems, which produces mechanical and thermal effects and facilitates mass transfer. When  $\text{CaCO}_3$  precipitation was carried out using ultrasounds, the vaterite concentration was higher compared to the process using the same reagent mixed by a magnetic stirrer. In the carbonation method using gaseous  $\text{CO}_2$ , mixing is generated by a gas flow. Therefore, an increase in the gas flow rate resulted in an increase in the vaterite precipitation [19,59,78,79].

### 5.6. Additives

The presence of additives in the reaction mixture may affect the precipitation by changing the solubility of a forming substance, influencing the reactive crystallization rate, nucleation, and crystal growth; the selective stabilization of a less stable polymorph; and the morphology of the forming crystals. The selected compounds that were additives in the reaction mixture used for the precipitation of calcium carbonate and their effect on the formation of vaterite are presented in Table 3.

The selection of the solvent for the precipitation of calcium carbonate has been intensively investigated. The addition of an organic solvent may change supersaturation [80], because usually both the solubility of each polymorphs and the activities of ions decreases. Therefore the promotion of vaterite precipitation in aqueous solutions of organic solvents is frequently reported [10,31,73,74]. Moreover, organic solvent and water molecules may be inhomogeneously dispersed. Such phenomena are observed, e.g., in ethanol-water mixtures, and are enhanced by an increase of the ethanol concentration and the addition of an inorganic salt [81]. Another feature of an aqueous ethanol solution is the ability to perform selective solvation as confirmed by a molecular dynamic simulation [81]. In this case, carbonate ions were mostly solvated by water and hardly solvated by ethanol, while calcium ions were solvated by both water ethanol molecules. These can lead to changes in the morphology of the precipitated particles of vaterite. As mentioned before, the addition of an organic solvent to the reaction mixture increases the supersaturation of the solution, hence the formation of vaterite particles considerably smaller in size is observed [10,74]. This is a result of the higher nucleation rate that provides a large number of nucleation sites in these systems. Moreover, organic solvent molecules that have negatively charged hydroxyl groups can adsorb at the forming vaterite surface, change the surface energy of the vaterite, and, as a result, stabilize these phases, thus preventing its transformation into more stable forms as has been reported for vaterite precipitation using the solvothermal method [23].

The formation of the adsorption layer at the produced crystals at the early stage of precipitation by different organic molecules added into the solution is often raised in the discussion of the role of organic additives. The adsorbed layer can inhibit the dissolution step of vaterite that is attributed to the remaining more unstable phases. If the adsorption energy of organic molecules at the solid surface interface is not enough to overcome the hydration energy of the hydrophilic part of these molecules,

they are removed from the crystal surface. Then, the precipitated vaterite is re-dissolved into water and a more stable calcite is formed by the recrystallization process [82].

**Table 3.** The influence of selective additives on vaterite precipitation.

| Additive                                    | Synthesis Method                   | Influence |           |            |      | Ref. |
|---|------------------------------------|-----------|-----------|------------|------|------|
|   |                                    | Rate      | Stability | Morphology | Size |      |
| Ethanol                                     | L-L, t = 25 °C                     | +         | +         | +          | +    | [31] |
|   | L-L, t = 25–30 °C                  |           |           |            |      | [81] |
| Iso-propanol                                | L-L, t = 25 °C                     | +         | +         | +          | +    | [31] |
|   | L-L, t = 25–30 °C                  |           |           |            |      | [81] |
| Diethylene glycol                           | L-L, t = 25 °C                     | +         | +         | +          | +    | [31] |
| Ethylene glycol                             | L-L, t = 2–40 °C                   | +         | +         | +          | +    | [10] |
|   | L-L, t = 25–80 °C                  |           |           |            |      | [73] |
|   | L-L, t = 25–50 °C                  |           |           |            |      | [47] |
|   | L-L, t = 40, 70 °C                 |           |           |            |      | [80] |
|   | Solv., t = 100–150 °C              |           |           |            |      | [23] |
| Glycerol                                    | L-L, t = 2–40 °C                   | +         | +         | +          | +    | [10] |
|   | Solv., t = 100–150 °C              |           |           |            |      | [23] |
| Erythritol                                  | L-L, t = 2–40 °C                   |           | +         |            | +    | [10] |
| 1,2-propanediol                             | Solv., t = 100–150 °C              |           | +         |            |      | [23] |
| 1,8-diaminooctane                           | G-S; t = 30 °C                     | +         |           |            |      | [82] |
| Glycine                                     | L-L, Diff., t <sub>a</sub>         | +         |           | +          |      | [52] |
|   | G-S; t = 30 °C                     |           |           |            |      | [82] |
| 4-aminobutyric acid<br>6-aminohexanoic acid | G-S; t = 30 °C                     | +         |           |            |      | [82] |
|   |                                    | +         |           |            |      |      |
| Poly-glutamic acid<br>Poly-aspartic acid    | L-L, t = 25 °C                     | +         |           | +          |      | [33] |
|   |                                    | +         |           | +          |      |      |
| Oleic acid                                  | L-L, t = 30 °C                     |           | +         |            |      | [83] |
| EDTMPA                                      | G-L, t = 30, 60 °C                 |           |           | +          | +    | [84] |
| Sucrose                                     | L-L, t = 30 °C                     | +         |           | +          |      | [50] |
|   | G-L, t = 22 °C                     |           |           |            |      | [85] |
| SDSN<br>SDBS                                | CaCl <sub>2</sub> +urea; t = 90 °C |           |           | +          | +    | [66] |
|   |                                    |           |           |            |      |      |
| Tween 20                                    | L-L, t <sub>a</sub>                |           |           | +          |      | [49] |
| Tween 40                                    |                                    |           |           |            |      |      |
| Tween 60                                    |                                    |           |           |            |      |      |
| Tween 80                                    |                                    |           |           |            |      |      |
| Ionic liquid surfactant                     | L-L, t = 25 °C                     |           | +         | +          |      | [47] |
| Guar gum                                    | L-L, t = 0, 20, 40 °C              |           |           | +          |      | [12] |

Abbreviations: Solv.—a solvothermal method; G-S—a gas-slurry system, t<sub>a</sub>—an ambient temperature; EDTMPA—ethylenediamine-tetrakis-N,N,N,N-(methylenephosphonic acid); SDSN—sodium dodecylsulfonate; SDBS—sodium dodecylbenzenesulfonate.

The stabilization of a vaterite polymorph was reported for alcohols, polyalcohols [10,23,31,81], and aminoacids [82,86]. Vaterite particles were produced in the presence of aminoacids. Both polar interactions from the hydrophilic groups of additives and the hydrophobic interactions due to the van der Waals forces from the hydrophobic alkyl groups play an important role in stabilizing vaterite particles [82]. The stabilizing effect of oleic acid molecules was also demonstrated and the adsorption of oleic acid at the vaterite surface was confirmed by FTIR analysis [83]. Also, tetrazole [61] and fulvic acid [34] were identified as compounds that were able to adsorb at the vaterite surface and retard vaterite dissolution. The stabilization of vaterite particles was also observed when polypeptides [33],

bovine serum albumin, or soluble starch [87] was added into the reaction mixture. Hydrophilic and hydrophobic parts are present in surfactant molecules, therefore, these molecules can easily adsorb on the hydrophilic surface of vaterite particles. In the same conditions, the vaterite polymorphic form was precipitated in the solution containing surfactant while calcite formation was favored in a medium without the addition of surfactant molecules [75,88]. Moreover, changes in the morphology of vaterite particles precipitated in the presence of surfactant were observed [49,66].

Polymeric substances were tested as additives in vaterite precipitation, as well. Polypeptides adsorbed at the interfaces of forming particles. They decreased in aggregation and changed the electrokinetic and morphological properties of the precipitate [33]. However the addition of the guar gum to the initial calcium chloride solution resulted in the production of hollow spherical vaterite particles [12]. However, core-shell vaterite microspheres composed of nanoparticles in the core and hexagonal nanoplates at the outer layer were precipitated using solutions of calcium chloride and ammonium carbonate with the addition of poly(styrene sulfonic acid) sodium salt [45]. When the synthesis was performed using a sodium carbonate solution as a carbonate source, vaterite microspheres covered by nanorods were precipitated [45].

The influence of additives on the rate of calcium carbonate precipitation was reported for some systems. In the solution method, it was found that the addition of ethylene glycol [80] reduced the precipitation rate. The retardation of crystal growth was observed when poly-aspartic acid and poly-glutamic acid were present in the solution [33]. In these systems, high supersaturation was preserved for a longer time and it resulted in a higher concentration of the vaterite phase in precipitated calcium carbonate. However, an increase in the vaterite growth was observed in the presence of ethanol, isopropanol, and diethylene glycol [31]. However, the stabilization of vaterite particles by organic solvent molecules prevented its transformation to more stable calcite. The opposite effect was found when citric acid was added [34]. Then, the precipitation was also slower, but the creation of calcite was privileged. It seems that the addition of citric acid increased the solubility of calcium carbonate and reduced the supersaturation in the system, which could result in the crystallization of calcite. However, when precipitation was carried out by carbonation of the calcium hydroxide suspension, the addition of amines, diamines, and amino acids resulted in a longer reaction time [82]. Vaterite was created when diaminoctane and amino acids were used. Although amino acids did not promote the CO<sub>2</sub> absorption and the formation of high supersaturation, their stabilizing effect on the vaterite was prevalent. On the other hand, the addition of sucrose into the initial solution of calcium chloride and ammonia reduced the reaction time [85]. Sucrose facilitated the absorption of CO<sub>2</sub> and caused the high supersaturation in the system, which promoted the creation of vaterite.

In summary, according to the Ostwald rule, the least stable vaterite precipitates first and subsequently transforms to the more stable one. In the absence of an additive, the kinetics is a dominant factor influencing the vaterite concentration in the produced calcium carbonate. As additives can affect each stage of crystallization, i.e., nucleation, growth, and transformation, they can therefore change the course of the precipitation process. Comprehensive information on the influence of tested additives on vaterite precipitation is not available. As shown in Table 3, only one study presented the effects of the additive in three of the highlighted areas [31]. Little information is available for carbonation-based precipitation, where additional substances can also affect the rate of CO<sub>2</sub> absorption and the generation of supersaturation in the system.

## 6. Summary

Vaterite is a polymorphic form of calcium carbonate, which is the subject of many studies due to its unique properties and related potential applications. Especially, spherical polycrystalline particles of vaterite are indicated as the most promising ones for applications. Various utilizations require particles with defined characteristics to be obtained. In this review, methods used for spherical vaterite precipitation were presented. Classical routes and recently new proposed approaches for calcium



carbonate precipitation were summarized. Favorable conditions for vaterite particles precipitation were also described.

A variety of proposed methods allows the selection of an approach due to the availability of substrates and equipment, which may have an impact on the cost of the produced calcium carbonate. The problem of separating the obtained particles, e.g., in the emulsion method, is not discussed, but it may decide on the choice of a specific method. Also, the recovery or recirculation of the liquid residue has not been investigated so far.

Spherical vaterite particles can be formed using the presented methods when appropriate process parameters are maintained. The most frequently indicated conditions conducive to the formation of vaterite are the relatively high supersaturation, temperatures up to 40°C, and pH between 8 and 10. However, these parameters can be shifted because there are many relationships between them that are not fully understood. In particular, the presence of additives may affect the range of conditions favorable to the precipitation of vaterite. Therefore, the stabilizing role of additives seems to be a promising research area. Especially, the selection of non-toxic compounds is very important when vaterite particles are used in pharmaceutical and cosmetic preparations or for biomedical applications.

**Funding:** The research described in this paper was financially supported by Faculty of Chemistry, Gdansk University of Technology, grant number DS 033155.

**Conflicts of Interest:** The author declares no conflict of interest.

## References

1. Friedman, G.M.; Schultz, D.J. Precipitation of vaterite (CaCO<sub>3</sub>) during oil field drilling. *Mineral. Mag.* **1994**, *58*, 401–408. [[CrossRef](#)]
2. Anthony, J.W.; Bideaux, R.A.; Bladh, K.W.; Nichols, M.C. *Handbook of Mineralogy*; MDP Inc.: Chantilly, VA, USA, 2003; Volume 5.
3. Jones, B. Review of calcium carbonate polymorph precipitation in spring systems. *Sediment. Geol.* **2017**, *353*, 64–75. [[CrossRef](#)]
4. Berman, A. Biomineralization of Calcium Carbonate. The Interplay with Biosubstrates. In *Metal Ions Life Sciences, Vol. 4*; Sigel, A., Freisinger, E., Sigel, R.K.O., Eds.; J. Wiley & Sons Ltd., 2008; pp. 167–205.
5. Chakoumakos, B.C.; Pracheil, B.M.; Koenigs, R.P.; Bruch, R.M.; Feygenson, M. Empirically testing vaterite structural models using neutron diffraction and thermal analysis. *Sci. Rep.* **2016**, *6*, 36799. [[CrossRef](#)]
6. Falini, G.; Fermani, S.; Reggi, M.; Njegić Džakula, B.; Kralj, D. Evidence of structural variability among synthetic and biogenic vaterite. *Chem. Commun.* **2014**, *50*, 15370–15373. [[CrossRef](#)] [[PubMed](#)]
7. Schenk, A.S.; Albarracin, E.J.; Kim, Y.Y.; Ihli, J.; Meldrum, F.C. Confinement stabilises single crystal vaterite rods. *Chem. Commun.* **2014**, *50*, 4729–4732. [[CrossRef](#)]
8. Portugal, S.J.; Bowen, J.; Riehl, C. A rare mineral, vaterite, acts as a shock absorber in the eggshell of a communally nesting bird. *Ibis* **2018**, *160*, 173–178. [[CrossRef](#)]
9. Wightman, R.; Wallis, S.; Aston, P. Leaf margin organisation and the existence of vaterite-producing hydathodes in the alpine plant *Saxifraga scardica*. *Flora Morphol. Distrib. Funct. Ecol. Plants* **2018**, *241*, 27–34. [[CrossRef](#)]
10. Trushina, D.B.; Bukreeva, T.V.; Antipina, M.N. Size-Controlled Synthesis of Vaterite Calcium Carbonate by the Mixing Method: Aiming for Nanosized Particles. *Cryst. Growth Des.* **2016**, *16*, 1311–1319. [[CrossRef](#)]
11. Volodkin, D. CaCO<sub>3</sub> templated micro-beads and -capsules for bioapplications. *Adv. Colloid Interface Sci.* **2014**, *207*, 306–324. [[CrossRef](#)] [[PubMed](#)]
12. Yang, H.; Wang, Y.; Liang, T.; Deng, Y.; Qi, X.; Jiang, H.; Wu, Y.; Gao, H. Hierarchical porous calcium carbonate microspheres as drug delivery vector. *Prog. Nat. Sci. Mater. Int.* **2017**, *27*, 674–677. [[CrossRef](#)]
13. Svenskaya, Y.I.; Fattah, H.; Zakharevich, A.M.; Gorin, D.A.; Sukhorukov, G.B.; Parakhonskiy, B.V. Ultrasonically assisted fabrication of vaterite submicron-sized carriers. *Adv. Powder Technol.* **2016**, *27*, 618–624. [[CrossRef](#)]
14. Trofimov, A.D.; Ivanova, A.A.; Zyuzin, M.V.; Timin, A.S. Porous inorganic carriers based on silica, calcium carbonate and calcium phosphate for controlled/modulated drug delivery: Fresh outlook and future perspectives. *Pharmaceutics* **2018**, *10*, 167. [[CrossRef](#)] [[PubMed](#)]

15. Trushina, D.B.; Bukreeva, T.V.; Kovalchuk, M.V.; Antipina, M.N. CaCO<sub>3</sub> vaterite microparticles for biomedical and personal care applications. *Mater. Sci. Eng. C* **2015**, *45*, 644–658. [[CrossRef](#)]
16. Vogel, R.; Persson, M.; Feng, C.; Parkin, S.J.; Nieminen, T.A.; Wood, B.; Heckenberg, N.R.; Rubinsztein-Dunlop, H. Synthesis and surface modification of birefringent vaterite microspheres. *Langmuir* **2009**, *25*, 11672–11679. [[CrossRef](#)]
17. Parkin, S.J.; Vogel, R.; Persson, M.; Funk, M.; Loke, V.L.Y.; Nieminen, T.A.; Heckenberg, N.R.; Rubinsztein-Dunlop, H. Highly birefringent vaterite microspheres: production, characterization and application for optical micromanipulation. *Opt. Express* **2009**, *17*, 721–727. [[CrossRef](#)] [[PubMed](#)]
18. Mori, Y.; Enomae, T.; Isogai, A. Application of Vaterite-Type Calcium Carbonate Prepared by Ultrasound for Ink Jet Paper. *J. Imaging Sci. Technol.* **2010**, *54*, 020504-1–020504-6. [[CrossRef](#)]
19. Udrea, I.; Capat, C.; Olaru, E.A.; Isopescu, R.; Mihai, M.; Mateescu, C.D.; Bradu, C. Vaterite synthesis via gas-liquid route under controlled pH conditions. *Ind. Eng. Chem. Res.* **2012**, *51*, 8185–8193. [[CrossRef](#)]
20. Nehrke, G.; Van Cappellen, P. Framboidal vaterite aggregates and their transformation into calcite: A morphological study. *J. Cryst. Growth* **2006**, *287*, 528–530. [[CrossRef](#)]
21. Tai, C.Y.; Chen, F.B. Polymorphism of CaCO<sub>3</sub>, precipitated in a constant-composition environment. *AIChE J.* **1998**, *44*, 1790–1798. [[CrossRef](#)]
22. Zhan, J.; Lin, H.-P.; Mou, C.-Y. Biomimetic Formation of Porous Single-Crystalline CaCO<sub>3</sub> via Nanocrystal Aggregation. *Adv. Mater.* **2003**, *15*, 621–623. [[CrossRef](#)]
23. Li, Q.; Ding, Y.; Li, F.; Xie, B.; Qian, Y. Solvothermal growth of vaterite in the presence of ethylene glycol, 1,2-propanediol and glycerin. *J. Cryst. Growth* **2002**, *236*, 357–362. [[CrossRef](#)]
24. Chen, J.; Xiang, L. Controllable synthesis of calcium carbonate polymorphs at different temperatures. *Powder Technol.* **2009**, *189*, 64–69. [[CrossRef](#)]
25. Kawano, J.; Shimobayashi, N.; Miyake, A.; Kitamura, M. Precipitation diagram of calcium carbonate polymorphs: Its construction and significance. *J. Phys. Condens. Matter* **2009**, *41*, 425102. [[CrossRef](#)]
26. Tas, A.C. Monodisperse calcium carbonate microtablets forming at 70°C in prerefrigerated CaCl<sub>2</sub>-Gelatin-Urea solutions. *Int. J. Appl. Ceram. Technol.* **2009**, *6*, 53–59. [[CrossRef](#)]
27. Christy, A.G. A Review of the Structures of Vaterite: The Impossible, the Possible, and the Likely. *Cryst. Growth Des.* **2017**, *17*, 3567–3578. [[CrossRef](#)]
28. Burgess, K.M.N.; Bryce, D.L. On the crystal structure of the vaterite polymorph of CaCO<sub>3</sub>: A calcium-43 solid-state NMR and computational assessment. *Solid State Nucl. Magn. Reson.* **2015**, *65*, 75–83. [[CrossRef](#)]
29. Plummer, N.L.; Busenberg, E. The solubilities of calcite, aragonite and vaterite in CO<sub>2</sub>-H<sub>2</sub>O solutions between 0 and 90°C, and an evaluation of the aqueous model for the system CaCO<sub>3</sub>-CO<sub>2</sub>-H<sub>2</sub>O. *Geochim. Cosmochim. Acta* **1982**, *46*, 1011–1040. [[CrossRef](#)]
30. Ševčík, R.; Šašek, P.; Viani, A. Physical and nanomechanical properties of the synthetic anhydrous crystalline CaCO<sub>3</sub> polymorphs: vaterite, aragonite and calcite. *J. Mater. Sci.* **2018**, *53*, 4022–4033. [[CrossRef](#)]
31. Manoli, F.; Dalas, E. Spontaneous precipitation of calcium carbonate in the presence of ethanol, isopropanol and diethylene glycol. *J. Cryst. Growth* **2000**, *218*, 359–364. [[CrossRef](#)]
32. Barhoum, A.; Ibrahim, H.M.; Hassanein, T.F.; Hill, G.; Reniers, F.; Dufour, T.; Delplancke, M.P.; Van Assche, G.; Rahier, H. Preparation and characterization of ultra-hydrophobic calcium carbonate nanoparticles. *IOP Conf. Ser. Mater. Sci. Eng.* **2014**, *64*, 012037. [[CrossRef](#)]
33. Njegić-Džakula, B.; Falini, G.; Brečević, L.; Skoko, Ž.; Kralj, D. Effects of initial supersaturation on spontaneous precipitation of calcium carbonate in the presence of charged poly-l-amino acids. *J. Colloid Interface Sci.* **2010**, *343*, 553–563. [[CrossRef](#)] [[PubMed](#)]
34. Vdović, N.; Kralj, D. Electrokinetic properties of spontaneously precipitated calcium carbonate polymorphs: The influence of organic substances. *Colloids Surfaces A Physicochem. Eng. Asp.* **2000**, *161*, 499–505. [[CrossRef](#)]
35. Perić, J.; Vučak, M.; Krstulović, R.; Brečević, L.; Kralj, D. Phase transformation of calcium carbonate polymorphs. *Thermochim. Acta* **1996**, *277*, 175–186. [[CrossRef](#)]
36. Nassrallah-Aboukaïs, N.; Jacquemin, J.; Decarne, C.; Abi-Aad, E.; Lamonier, J. F.; Aboukaïs, A. Transformation of vaterite into calcite in the absence and the presence of copper(II) species. Thermal analysis, IR and EPR study. *J. Therm. Anal. Calorim.* **2003**, *74*, 21–27. [[CrossRef](#)]
37. Wolf, G.; Günther, C. Thermophysical investigations of the polymorphous phases of calcium carbonate. *J. Therm. Anal. Calorim.* **2001**, *65*, 687–698. [[CrossRef](#)]

38. Maruyama, K.; Kagi, H.; Komatsu, K.; Yoshino, T.; Nakano, S. Pressure-induced phase transitions of vaterite, a metastable phase of CaCO<sub>3</sub>. *J. Raman Spectrosc.* **2017**, *48*, 1449–1453. [[CrossRef](#)]
39. Vagenas, N.V.; Gatsouli, A.; Kontoyannis, C.G. Quantitative analysis of synthetic calcium carbonate polymorphs using FT-IR spectroscopy. *Talanta* **2003**, *59*, 831–836. [[CrossRef](#)]
40. Kontoyannis, C.G.; Vagenas, N.V. Calcium carbonate phase analysis using XRD and FT-Raman spectroscopy. *Analyst* **2000**, *125*, 251–255. [[CrossRef](#)]
41. Bryce, D.L.; Bultz, E.B.; Aebi, D. Calcium-43 chemical shift tensors as probes of calcium binding environments. Insight into the structure of the vaterite CaCO<sub>3</sub> polymorph by <sup>43</sup>Ca solid-state NMR spectroscopy. *J. Am. Chem. Soc.* **2008**, *130*, 9282–9292. [[CrossRef](#)]
42. Rodriguez-Blanco, J.D.; Shaw, S.; Benning, L.G. The kinetics and mechanisms of amorphous calcium carbonate (ACC) crystallization to calcite, viavaterite. *Nanoscale* **2011**. [[CrossRef](#)]
43. Gebauer, D.; Gunawidjaja, P.N.; Ko, J.Y.P.; Bacsik, Z.; Aziz, B.; Liu, L.; Hu, Y.; Bergström, L.; Tai, C.W.; Sham, T.K.; Edén, M.; Hedin, N. Proto-calcite and proto-vaterite in amorphous calcium carbonates. *Angew. Chem. Int. Ed.* **2010**, *49*, 8889–8891. [[CrossRef](#)] [[PubMed](#)]
44. Andreassen, J.-P.; Lewis, A.E. Classical and Nonclassical Theories of Crystal Growth. In *New Perspectives on Mineral Nucleation and Growth*; van Driessche, A., Kellermeier, M., Benning, L.G., Gebauer, D., Eds.; Springer International Publishing Switzerland: Cham, Switzerland, 2017; pp. 137–154.
45. Yang, M.; Jin, X.; Huang, Q. Facile synthesis of vaterite core-shell microspheres. *Colloids Surfaces A Physicochem. Eng. Asp.* **2011**, *374*, 102–107. [[CrossRef](#)]
46. Zhao, D.; Jiang, J.; Xu, J.; Yang, L.; Song, T.; Zhang, P. Synthesis of template-free hollow vaterite CaCO<sub>3</sub> microspheres in the H<sub>2</sub>O/EG system. *Mater. Lett.* **2013**, *104*, 28–30. [[CrossRef](#)]
47. Andreassen, J.P.; Flaten, E.M.; Beck, R.; Lewis, A.E. Investigations of spherulitic growth in industrial crystallization. *Chem. Eng. Res. Des.* **2010**, *88*, 1163–1168. [[CrossRef](#)]
48. Andreassen, J.-P. Formation mechanism and morphology in precipitation of vaterite-nano-aggregation or crystal growth? *J. Cryst. Growth* **2005**, *274*, 256–264. [[CrossRef](#)]
49. Mori, Y.; Enomae, T.; Isogai, A. Preparation of pure vaterite by simple mechanical mixing of two aqueous salt solutions. *Mater. Sci. Eng. C* **2009**, *29*, 1409–1414. [[CrossRef](#)]
50. Mahtout, L.; Sánchez-Soto, P.J.; Carrasco-Hurtado, B.; Pérez-Villarejo, L.; Takabait, F.; Eliche-Quesada, D. Synthesis of vaterite CaCO<sub>3</sub> as submicron and nanosized particles using inorganic precursors and sucrose in aqueous medium. *Ceram. Int.* **2018**, *44*, 5291–5296. [[CrossRef](#)]
51. Jiang, J.; Zhao, H.; Wang, X.; Xiao, B.; Chen, C.; Wu, Y.; Yang, C.; Xu, S. A novel route to prepare the metastable vaterite phase of CaCO<sub>3</sub> from CaCl<sub>2</sub> ethanol solution and Na<sub>2</sub>CO<sub>3</sub> aqueous solution. *Adv. Powder Technol.* **2018**, *29*, 2416–2422. [[CrossRef](#)]
52. Hou, W.; Feng, Q. Morphology and formation mechanism of vaterite particles grown in glycine-containing aqueous solutions. *Mater. Sci. Eng. C* **2006**, *26*, 644–647. [[CrossRef](#)]
53. Chen, Y.; Ji, X.; Wang, X. Microwave-assisted synthesis of spheroidal vaterite CaCO<sub>3</sub> in ethylene glycol-water mixed solvents without surfactants. *J. Cryst. Growth* **2010**, *312*, 3191–3197. [[CrossRef](#)]
54. Svenskaya, Y.I.; Fattah, H.; Inozemtseva, O.A.; Ivanova, A.G.; Shtykov, S.N.; Gorin, D.A.; Parakhonskiy, B.V. Key Parameters for Size- and Shape-Controlled Synthesis of Vaterite Particles. *Cryst. Growth Des.* **2018**, *18*, 331–337. [[CrossRef](#)]
55. Han, Y.S.; Hadiko, G.; Fuji, M.; Takahashi, M. Crystallization and transformation of vaterite at controlled pH. *J. Cryst. Growth* **2006**, *289*, 269–274. [[CrossRef](#)]
56. Popescu, M.A.; Isopescu, R.; Matei, C.; Fagarasan, G.; Plesua, V. Thermal decomposition of calcium carbonate polymorphs precipitated in the presence of ammonia and alkylamines. *Adv. Powder Technol.* **2014**, *25*, 500–507. [[CrossRef](#)]
57. Konopacka-Lyskawa, D.; Kościelska, B.; Karczewski, J.; Gołębiewska, A. The influence of ammonia and selected amines on the characteristics of calcium carbonate precipitated from calcium chloride solutions via carbonation. *Mater. Chem. Phys.* **2017**, *193*, 13–18. [[CrossRef](#)]
58. Prah, J.; Maček, J.; Dražič, G. Precipitation of calcium carbonate from a calcium acetate and ammonium carbamate batch system. *J. Cryst. Growth* **2011**, *324*, 229–234. [[CrossRef](#)]
59. Sun, J.; Wang, L.; Zhao, D. Polymorph and morphology of CaCO<sub>3</sub> in relation to precipitation conditions in a bubbling system. *Chin. J. Chem. Eng.* **2017**, *25*, 1335–1342. [[CrossRef](#)]

60. Donnelly, F.C.; Purcell-Milton, F.; Framont, V.; Cleary, O.; Dunne, P.W.; Gun'ko, Y.K. Synthesis of CaCO<sub>3</sub> nano- and micro-particles by dry ice carbonation. *Chem. Commun.* **2017**, *53*, 6657–6660. [[CrossRef](#)] [[PubMed](#)]
61. Massi, M.; Ogden, M.I.; Jones, F. Investigating vaterite phase stabilisation by a tetrazole molecule during calcium carbonate crystallisation. *J. Cryst. Growth* **2012**, *351*, 107–114. [[CrossRef](#)]
62. Lyu, S.G.; Park, S.; Sur, G.S. The Synthesis of Vaterite and Physical Properties of PP/CaCO<sub>3</sub> Composites. *Korean J. Chem. Eng.* **1999**, *16*, 538–542. [[CrossRef](#)]
63. Hirai, T.; Hariguchi, S.; Komasa, I.; Davey, R.J. Biomimetic Synthesis of Calcium Carbonate Particles in a Pseudovesicular Double Emulsion. *Langmuir* **2002**, *13*, 6650–6653. [[CrossRef](#)]
64. Ganguli, A.K.; Ahmad, T.; Vaidya, S.; Ahmed, J. Microemulsion route to the synthesis of nanoparticles. *Pure Appl. Chem.* **2008**, *80*, 2451–5477. [[CrossRef](#)]
65. Walsh, D.; Lebeau, B.; Mann, S. Morphosynthesis of calcium carbonate (vaterite) microsponges. *Adv. Mater.* **1999**, *11*, 324–328. [[CrossRef](#)]
66. Huang, J.H.; Mao, Z.F.; Luo, M.F. Effect of anionic surfactant on vaterite CaCO<sub>3</sub>. *Mater. Res. Bull.* **2007**, *42*, 2184–2191. [[CrossRef](#)]
67. Wang, L.; Sondi, I.; Matijević, E. Preparation of Uniform Needle-Like Aragonite Particles by Homogeneous Precipitation. *J. Colloid Interface Sci.* **1999**, *218*, 545–553. [[CrossRef](#)]
68. Gopi, S.; Subramanian, V.K.; Palanisamy, K. Aragonite-calcite-vaterite: A temperature influenced sequential polymorphic transformation of CaCO<sub>3</sub> in the presence of DTPA. *Mater. Res. Bull.* **2013**, *48*, 1906–1912. [[CrossRef](#)]
69. Kitamura, M. Strategy for control of crystallization of polymorphs. *CrystEngComm* **2009**, *11*, 949–964. [[CrossRef](#)]
70. Beck, R.; Andreassen, J.P. The onset of spherulitic growth in crystallization of calcium carbonate. *J. Cryst. Growth* **2010**, *312*, 2226–2238. [[CrossRef](#)]
71. Vučak, M.; Perić, J.; Krstulović, R. Precipitation of calcium carbonate in a calcium nitrate and monoethanolamine solution. *Powder Technol.* **1997**, *91*, 69–74. [[CrossRef](#)]
72. Ogino, T.; Suzuki, T.; Sawada, K. The formation and transformation mechanism of calcium carbonate in water. *Geochim. Cosmochim. Acta* **1987**, *51*, 2757–2767. [[CrossRef](#)]
73. Flaten, E.M.; Seiersten, M.; Andreassen, J.P. Polymorphism and morphology of calcium carbonate precipitated in mixed solvents of ethylene glycol and water. *J. Cryst. Growth* **2009**, *311*, 3533–3538. [[CrossRef](#)]
74. Oral, Ç.M.; Ercan, B. Influence of pH on morphology, size and polymorph of room temperature synthesized calcium carbonate particles. *Powder Technol.* **2018**, *339*, 781–788. [[CrossRef](#)]
75. Zhao, Y.; Du, W.; Sun, L.; Yu, L.; Jiao, J.; Wang, R. Facile synthesis of calcium carbonate with an absolutely pure crystal form using 1-butyl-3-methylimidazolium dodecyl sulfate as the modifier. *Colloid Polym. Sci.* **2013**, *291*, 2129–2202. [[CrossRef](#)]
76. Bots, P.; Benning, L.G.; Rodriguez-Blanco, J.-D.; Roncal-Herrero, T.; Shaw, S. Mechanistic Insights into the Crystallization of Amorphous Calcium Carbonate (ACC). *Cryst. Growth Des.* **2012**, *12*, 3806–3814. [[CrossRef](#)]
77. Kralj, D.; Brecević, L.; Nielsen, A.E. Vaterite growth and dissolution in aqueous solution II. Kinetics of dissolution. *J. Cryst. Growth* **1994**, *143*, 269–276. [[CrossRef](#)]
78. Isopescu, R.; Mîhai, M.; Căpat, C.; Olaru, A.; Mateescu, C.; Dumitrescu, O.; Udrea, I. Modelling of Calcium Carbonate Synthesis by Gas-Liquid Reaction Using CO<sub>2</sub> from Flue Gases. *Chem. Eng. Trans.* **2011**, *25*, 713–718. [[CrossRef](#)]
79. Konopacka-Lyskawa, D.; Kościelska, B.; Łapiński, M. Precipitation of Spherical Vaterite Particles via Carbonation Route in the Bubble Column and the Gas-Lift Reactor. *JOM* **2019**, *71*, 1041–1048. [[CrossRef](#)]
80. Flaten, E.M.; Seiersten, M.; Andreassen, J.P. Growth of the calcium carbonate polymorph vaterite in mixtures of water and ethylene glycol at conditions of gas processing. *J. Cryst. Growth* **2010**, *312*, 953–960. [[CrossRef](#)]
81. Zhang, L.; Yue, L.H.; Wang, F.; Wang, Q. Divisive effect of alcohol-water mixed solvents on growth morphology of calcium carbonate crystals. *J. Phys. Chem. B* **2008**, *112*, 10668–10674. [[CrossRef](#)] [[PubMed](#)]
82. Chuaiji, W.; Takatori, K.; Igarashi, T.; Hara, H.; Fukushima, Y. The influence of aliphatic amines, diamines, and amino acids on the polymorph of calcium carbonate precipitated by the introduction of carbon dioxide gas into calcium hydroxide aqueous suspensions. *J. Cryst. Growth* **2014**, *386*, 119–127. [[CrossRef](#)]
83. Wang, C.; Piao, C.; Zhai, X.; Hickman, F.N.; Li, J. Synthesis and character of super-hydrophobic CaCO<sub>3</sub> powder in situ. *Powder Technol.* **2010**, *200*, 84–86. [[CrossRef](#)]

84. Vucak, M.; Peric, J.; Pons, M.-N. The Influence of Various Admixtures on the Calcium Carbonate Precipitation from a Calcium Nitrate and Monoethanolamine Solution. *Chem. Eng. Technol.* **1998**, *21*, 71–75. [[CrossRef](#)]
85. Konopacka-Lyskawa, D.; Czaplicka, N.; Kościelska, B.; Łapiński, M.; Gębicki, J. Influence of Selected Saccharides on the Precipitation of Calcium-Vaterite Mixtures by the CO<sub>2</sub> Bubbling Method. *Crystals* **2019**, *9*, 117. [[CrossRef](#)]
86. Štajner, L.; Kontrec, J.; NjegićDžakula, B.; Maltar-Strmečki, N.; Plodinec, M.; Lyons, D.M.; Kralj, D. The effect of different amino acids on spontaneous precipitation of calcium carbonate polymorphs. *J. Cryst. Growth* **2018**, *486*, 71–81. [[CrossRef](#)]
87. Liu, Y.; Chen, Y.; Huang, X.; Wu, G. Biomimetic synthesis of calcium carbonate with different morphologies and polymorphs in the presence of bovine serum albumin and soluble starch. *Mater. Sci. Eng. C* **2017**, *79*, 457–464. [[CrossRef](#)] [[PubMed](#)]
88. Płaza, G.; Legawiec, K.; Bastrzyk, A.; Fiedot-Toboła, M.; Polowczyk, I. Effect of a lipopeptide biosurfactant on the precipitation of calcium carbonate. *Colloids Surfaces B Biointerfaces* **2018**. [[CrossRef](#)]



© 2019 by the author. Licensee MDPI, Basel, Switzerland. This article is an open access article distributed under the terms and conditions of the Creative Commons Attribution (CC BY) license (<http://creativecommons.org/licenses/by/4.0/>).